Available online at www.sciencedirect.com

SciVerse ScienceDirect

Journal of the European Ceramic Society 32 (2012) 1551–1559

www.elsevier.com/locate/jeurceramsoc

# Influence of ultra-high residual compressive stress on the static and dynamic indentation response of a chemically strengthened glass

Phillip Jannotti [a], Ghatu Subhash [a,*], Peter Ifju [a], Patrick K. Kreski [b], Arun K. Varshneya [b]

[a] *Mechanical & Aerospace Engineering, University of Florida, Gainesville, FL 32611, United States*
[b] *Saxon Glass Technologies, Inc., Alfred, NY 14802, United States*

Received 19 July 2011; received in revised form 13 December 2011; accepted 5 January 2012
Available online 30 January 2012

**Abstract**

The influence of ultra-high surface compressive stresses (∼1 GPa) on the static and dynamic indentation response was investigated on an ion-exchanged glass and compared with the raw glass properties. Static hardness measurements were conducted utilizing a standard Vickers hardness tester (15 s duration), while dynamic hardness measurements were performed using a custom-made dynamic indentation hardness tester (60 μs duration). It was found that there is an 11% increase in static and dynamic hardness from the raw glass to the strengthened glass due to chemical strengthening. The dynamic hardness on the strengthened glass was also 23% greater than the static hardness. Additionally, the strengthened glass exhibited notable radial crack suppression. To examine the subsurface hardness profile, static Vickers indentations were conducted on a lateral surface which was polished to remove the strengthened layer. The hardness profile revealed that the effect of strengthening extended to 3 times the case-depth measured using photoelasticity.


*Keywords:* Hardness; Indentation; Residual stress; Strengthened glass; Ion exchange

## 1. Introduction

Chemically strengthened glasses are used in many civilian, aerospace and military applications where good optical transparency and mechanical strength are essential. Examples of such applications include window glasses for airplanes and automobiles, fracture-resistant screens for personal electronic devices (e.g. cell phones screens and flat panel TVs) and hurricane-resistant windows.[1] They are also employed as panels for solar energy harvesting units which need to resist severe environmental erosion including impacts due to hail storms, hurricanes, and tornados.[2] Recently, there has been an increased interest in high-strength glasses for armored vehicle windows and for military personnel visors. These glasses have been engineered to have high surface compressive stresses that promote resistance to premature cracking due to surface flaws. A brief description of the advantages and the disadvantages of the chemical strengthening process over the more traditional thermal tempering process have been discussed by Varshneya.[2]

To quantify the strengthening that results from the ion exchange process it is necessary to determine the mechanical properties of the strengthened material. A common material property that is easy to determine and has been shown to relate to the impact performance of an armor is indentation hardness. Indentation hardness has been related to dwell phenomena during the early part of projectile interaction with ceramic armor and consequently to significant blunting and erosion of the projectile.[3–7] Despite numerous attempts to relate ballistic performance to mechanical properties of armor materials, hardness is one of the only commonly agreed upon properties with strong correlation to ballistic performance.[6,8–10] Furthermore, because of the ease of implementation and cost-effectiveness of static indentation measurements, hardness has become a popular metric for material characterization.[11] However, this method does not capture the rate sensitive behavior of brittle materials due to the long loading duration (15 s) which results in quasi-static deformation. On the other hand, the use of dynamic hardness experiments[11,12] can provide such information by generating high-rate indentations which in turn can be used to gain insight

* Corresponding author. Tel.: +1 352 392 7005; fax: +1 352 392 7303.
*E-mail address:* subhash@ufl.edu (G. Subhash).

0955-2219/$ – see front matter © 2012 Elsevier Ltd. All rights reserved.
doi:10.1016/j.jeurceramsoc.2012.01.002

into the effects of strain rate on hardness and indentation-induced damage.

Literature exists of indentation studies examining the influence of residual stress on hardness,[13,14] but these studies do not address the rate sensitivity of hardness due to residual stresses. Various investigations have been performed to examine the static and dynamic Vickers hardness of ceramics and brittle materials,[11,12,15–18] but little is known of the rate-sensitive indentation behavior of strengthened glasses such as Ion-Armor™. Furthermore, a number of studies have explored the residual stress profile with depth resulting from the strengthening process,[2,19–21] but, to the best of our knowledge little is known with regard to the subsurface hardness profile as a function of depth for a strengthened glass with ultra-high residual compressive stresses. Such studies allow for the determination of the extent of the surface strengthening process and the influence of resulting residual stress on the measured hardness values.

In the current study, indentation experiments were utilized to both qualitatively and quantitatively assess the effects of ultra-high residual compressive stresses (due to ion exchange) on the static and dynamic indentation response of a new class of chemically strengthened glass, Ion-Armor™. This glass has been shown to attain a high level of surface compressive stress close to 1 GPa[19] and large case-depths up to 1 mm.[1] The variation in hardness with load, strain rate and depth (from the strengthened surface), as well as its indentation-induced fracture characteristics are examined to assess the utility of such glasses for applications where high transparency and strength are desired. Photoelasticity was employed to determine the subsurface residual stress profile with depth.

## 2. Materials

Rectangular bars of lithium aluminosilicate glass of dimensions 23 mm × 9.9 mm × 7.6 mm, shown in Fig. 1(a), were chemically strengthened in mixed molten salt baths of potassium ($K^+$) and sodium ($Na^+$) ions using a procedure discussed by Varshneya and Spinelli.[1] Recently, Jannotti et al.[19] conducted systematic photoelasticity studies and determined that the surface compressive stress reached ~1 GPa and strengthening depths extended up to 0.8 mm. Beyond this depth, it was revealed that an anomalous tensile stress maximum (44 MPa) was present before the tensile stress became constant at 37 MPa within the interior of the specimen.

Select surfaces, as shown in Fig. 1(a), were ground and polished off with the intent to remove the strengthened layer of glass material up to a depth of approximately 1 mm. These surfaces were referred to as "unstrengthened" surfaces so as to differentiate them from the raw (or as-received) glass. It has been verified by Saxon Glass Technologies that the polishing of the two opposite faces of the strengthened glass bars did not alter the residual stress distribution. Fig. 1(b) shows the photoelastic fringe patterns associated with the strengthened surfaces when viewed through the unstrengthened surface. A large number of fringes exist along the periphery of the glass, revealing a high level of stress and a severe stress gradient near the edge. More details of the stress profile and stress magnitudes will be presented in Section 4.4.

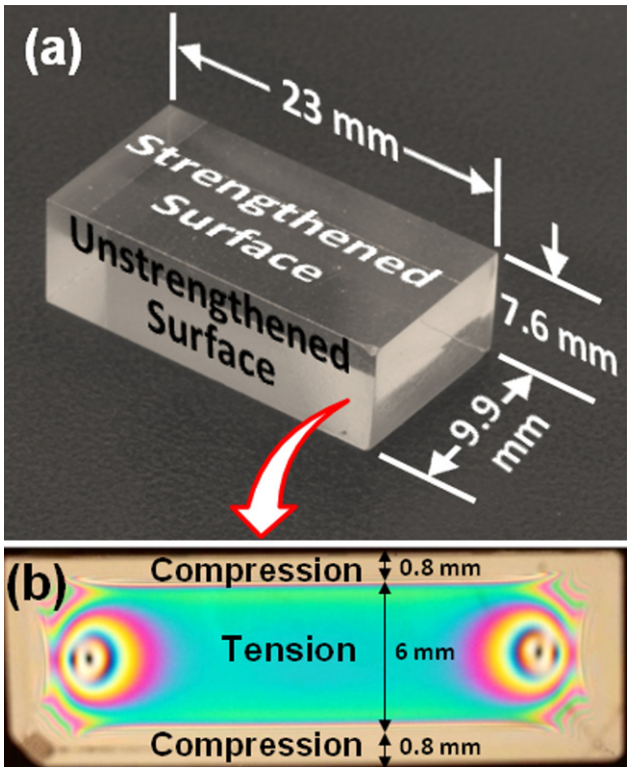


Fig. 1. (a) Image of the rectangular glass bars with strengthened and unstrengthened (polished) surfaces indicated and (b) isochromatic fringe patterns as viewed through the unstrengthened surface with a circular polariscope in dark-field arrangement.

## 3. Experimental procedure

Static and dynamic Vickers indentations were conducted to ascertain the influences of load, residual surface compressive stress and strain rate on the measured hardness values and indentation-induced damage evolution. A series of rows of static and dynamic indentations at a range of loads were made in the central regions of the strengthened and raw glass surfaces. Depending on the material surface being investigated an appropriate load range was chosen to generate Vickers indents while avoiding excessive cracking and material removal. Static hardness values were averaged based on at least 10 individual indents at a given load to provide a representative Vickers hardness value. The dynamic hardness values were not averaged because the load level for each indentation was different due to varying indenter velocities. For both static and dynamic indentation, the indent diagonal lengths and load (measured from the load cell) were used to determine the Vickers hardness.

The static Vickers indentation experiments were performed using a standard hardness tester (Wilson® Instruments Tukon™ model 2100B) with a Vickers diamond indenter tip. The loading duration of these indentations was approximately 15 s. This instrument had the ability to produce micro- as well as macro-Vickers indents with loads ranging from 50 g to 50 kg. The

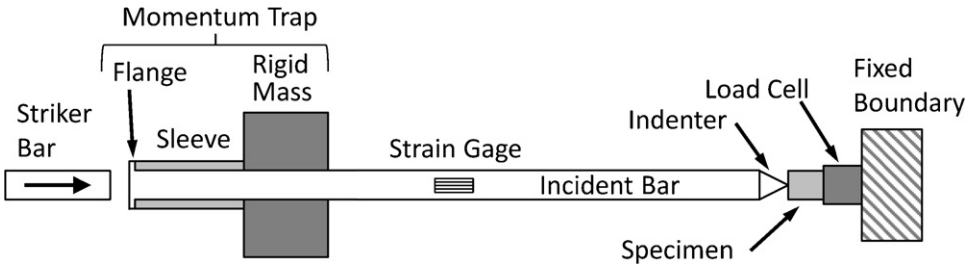


Fig. 2. Schematic of the dynamic indentation hardness tester (DIHT).

dynamic indentations were then performed using a custom-made dynamic indentation hardness tester (DIHT) as illustrated in Fig. 2. The utility and operating principles of dynamic indentation hardness measurements are well described on metals and ceramics in numerous publications by the corresponding author and research group,[11,12,15–18] therefore only a brief discussion is presented here. The DIHT consists of a long rod (or incident bar) with an indenter inserted at one end and a flange-sleeve-rigid mass assembly, also known as a momentum trap, at the other end.[24] The specimen whose hardness is to be determined is placed on top of a high frequency (∼200 kHz) load cell (Kistler model #9213). This load transducer is anchored to a rigid base. The indenter tip is brought into contact with the specimen before the dynamic indentation is performed. A striker bar is then launched from a gas gun towards the flanged-end of the incident bar. The impact of the striker generates a compressive stress wave followed by a tensile stress wave (due to the momentum trap) in the incident bar. The momentum trap ensures that only a single compressive pulse reaches the indenter tip and the rest of the waves are rendered tensile while traveling towards the indenter tip. Therefore, the indenter tip moves forward into the specimen only once, causing the desired indentation, and then retracts back in several incremental steps. Thus, a single indentation is achieved on the specimen within a short loading duration. The loading duration of indentation is proportional to the length of the striker bar, while the depth (or load) of indentation depends on the velocity of the striker bar. Typical loading durations using a 6 in. striker bar are on the order of 60 μs. A common question in such dynamic measurements is the strain rate of deformation. As is well known, the deformation within an indentation zone is highly non-uniform with the highest strains close to the indenter tip and gradually decreasing strains away from the tip. Therefore, an average strain rate is defined as the ratio of the indenter velocity to the average length of the indentation diagonals.[11,12] Typically, average strain rates are around 1000/s.

To investigate the hardness profile as a function of depth, static indentations were made from one edge to the other edge on both the strengthened and unstrengthened surfaces at a load of 4.91 N (0.5 kg). Rows consisting of five indents each were conducted at equally spaced intervals across the entire length of the surfaces. At each depth, the hardness values were averaged to provide a representative Vickers hardness value. Recall that the chemical strengthening of glass causes residual compressive stresses up to certain depth from the strengthened surface and that the unstrengthened surface has been polished to remove the strengthened layer. Because the residual stress state and magnitude of the stress change with depth from the strengthened surface, the hardness measured on the lateral surface (indicated as "unstrengthened" in Fig. 1) from one edge to the other should provide an indication of the extent and influence of the compressive stresses present from the strengthened surfaces down to a certain depth. Such a procedure is commonly employed in materials which have been case hardened.[22,23]

All Vickers indentations were examined using an optical microscope (Olympus model BX51) with Nomarski interference contrast capabilities. The indents were observed using both bright-field microscopy as well as differential interference contrast microscopy. All measurements of indentation diagonals were made immediately after each row of indents was completed. Measurement accuracy was ±∼3%. Also, note that all comparisons between measured hardness values on the strengthened and raw glass surfaces under static and dynamic loading were made at the same indentation load of 19.6 N (2 kg). The current analysis did not take into account the influences of pileup or sink-in. While there is ample literature on this topic, it is argued that for conventional Vickers hardness measurements, where the diagonals of the indentation (from corner to corner) are used for hardness determination, the effects of pileup and sink-in are diminished due to the geometrical constraint of the sharp indenter edges.[25]

Finally, a circular polariscope with white light and green filtered light (550 nm) was employed to image the photoelastic fringes patterns evolved due to the residual stresses in the Ion-Armor™ glass. Under white light, the colored fringes facilitated the detection of compressive and tensile stress regions as well as the zero order fringe (dark band) which represents the stress free zone. The zero order fringe also indicates the transition from compression to tension.[19] For low fringe orders, analysis under white light was appropriate; however, higher order fringes became diffused towards the edge of the specimen and the exact fringe order could not be accurately discerned. Therefore, a green optical bandpass filter (monochromatic light) was used while imaging the higher order fringes to improve image contrast. Nevertheless, the common problem in photoelastic measurements is a limitation in spatial resolution, especially in regions of severe stress gradients (high fringe density). This is easily resolved by minimizing the specimen thickness (in the viewing direction), which drastically improves the resolution. More details of this technique and analysis for the determination of the residual stress magnitude in Ion-Armor™ glass is given in Jannotti et al.[19]

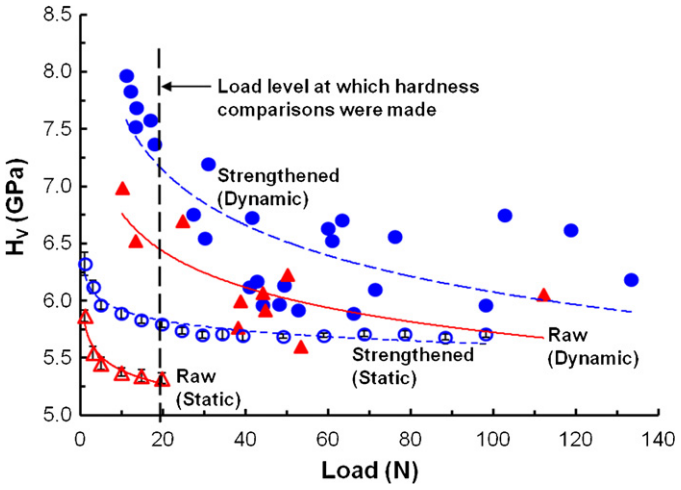


Fig. 3. Static and dynamic Vickers hardness data for various load ranges on the strengthened and raw glass surfaces. This data reveals ISE and significant increases in material hardness under dynamic loading for both surfaces.

## 4. Results and discussion

### 4.1. Static and dynamic hardness

The static and dynamic hardness values of the strengthened and the raw glass surfaces are plotted in Fig. 3. Static hardness values are denoted by open circles while dynamic hardness values are denoted by filled circles. It is important to note that unlike the static hardness data, each dynamic data point represents one hardness value at one specific load level (based on striker bar velocity). It is evident from the figure that all of the hardness measurements (static and dynamic) exhibited a load-dependence, known as the indentation size effect.[26,27] For brittle materials, the indentation size effect (ISE) is well documented.[11,28–31] The ISE is observed as a decrease in hardness with increasing indentation load. Beyond a certain load a constant hardness value is reached, but this specific load is material dependent. Although it was observed that the measured hardness began to level off once a certain indentation load was reached, incipient cracking at higher loads did not always allow for the determination of the exact load at which the hardness values became constant. This is a common concern while testing brittle materials due to their increased propensity for cracking.

After analyzing the hardness measurements as a function of load under static and dynamic indentation, definitive conclusions were drawn as to the beneficial effects of the ion exchange process on the indentation hardness. From Fig. 3 it was observed that the hardness of the strengthened surface was significantly higher than that of the raw glass. The strengthened surface showed an increase in both static and dynamic Vickers hardness of about 11% compared to the raw surface at a load of 19.6 N (2 kg). These findings are consistent with previous studies where compressive stresses were shown to result in elevated hardness values.[13,14,32]

The observed increases in static and dynamic hardness can be readily attributed to the high levels of residual compressive stress present on the strengthened glass surfaces. Recall that during the ion exchange process the surface of the ion exchanged glass is heavily flooded with larger $Na^+$ and $K^+$ ions. Due to the wedging of these larger ions into the glass matrix, large residual compressive stresses (determined to be close to 1 GPa[19]) were generated along the in-plane direction. Such high levels of in-plane residual compression can strongly resist the penetration of the indenter, giving rise to notably higher hardness values compared to that of the raw glass. Studies by Kese et al.[13] showed that compressive stresses can present a notable effect not only on the hardness, but also on the elastic modulus. As the elastic modulus was observed to exhibit proportionality to indentation hardness,[13] the increase in elastic modulus due to high levels of residual compression would then be expected to predict elevated values of hardness.

Similar improvements in hardness values were observed due to increased strain rate (see Fig. 3). The dynamic hardness of the strengthened glass was 23% greater than its static hardness. In addition, the hardness of the raw glass showed a 22% increase in hardness under dynamic loading compared to its static hardness. The enhancement of hardness observed under dynamic loading rates is a beneficial trait for a material that is intended to be used for resisting high-velocity impacts (i.e. solar panel covers in extreme desert environments or transparent armor applications). It further highlights the importance of material testing under high loading rates for materials intended for dynamic applications. These results are in line with established high strain rate literature on ceramics in which mechanical properties, such as Vickers hardness, were found to increase with loading rate.[17,18] Also note that the dynamic indentation hardness could be accurately determined at significantly higher load levels because of the reduced damage surrounding the dynamic Vickers imprint.

### 4.2. Damage evolution

By analyzing the optical micrographs of static and dynamic indentations, it was possible to assess the influences exhibited by residual stress and loading rate on the damage evolved under comparable indentation load levels. Fig. 4 illustrates a comparison of the indentation-induced damage patterns due to static indentations on strengthened and raw glass surfaces at the same load levels. The measured hardness and load level is also indicated on each micrograph. Under static loads, little or no damage/cracking is seen on the strengthened surface until a load of 9.81 N (1 kg) is reached, as evidenced by Fig. 4(a). Only minor edge cracks and shear fault lines were observed to run parallel to the edges of indentation impressions. On the other hand, the raw glass exhibited minor edge cracking at 2.94 N (0.3 kg) (not shown for brevity), as well as shear faulting, radial cracking and lateral cracking at 9.81 N (1 kg), as shown in Fig. 4(b). Most importantly, the results indicated that the presence of compressive surface stresses acted to suppress the appearance of radial cracking which was so prominent in the raw lithium aluminosilicate glass (see Fig. 4(b)).

Despite the sole influence of the residual compressive stress on the indentation response, it is important to examine the additional influences of strain rate on the observed indentation-induced damage progression. The micrographs

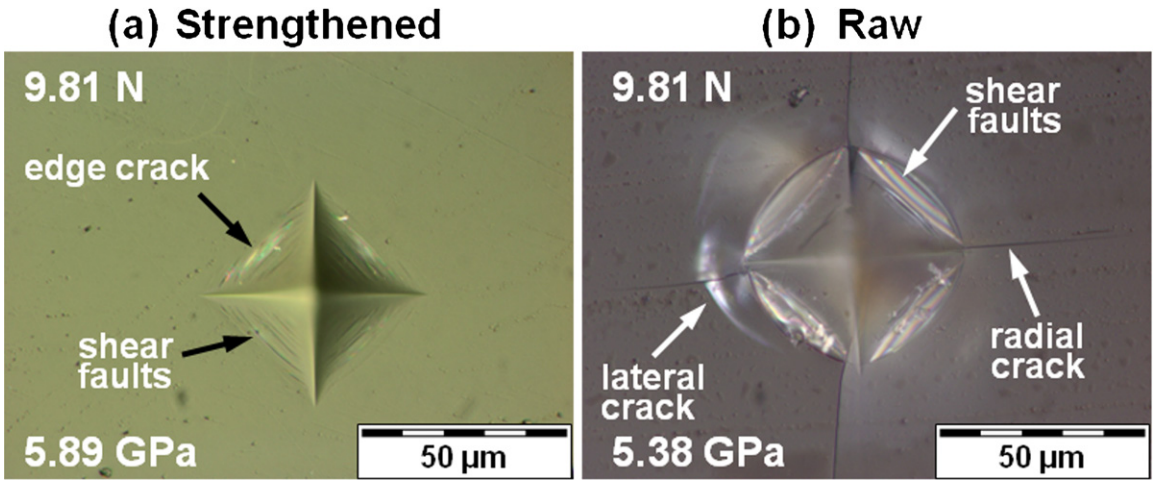


Fig. 4. Micrographs of static Vickers indents at a load of 9.81 N on (a) strengthened and (b) raw glass surfaces. Included on each micrograph is the load (top) and the average Vickers hardness value (bottom) for that load. Note the significant decrease in damage on the strengthened glass compared to the raw glass.

presented in Fig. 5 illustrate the damage evolved due to dynamic indentations. At a low load of 13.3 N (1.36 kg), the strengthened surface revealed minimal crack development. Only minor edge cracks and shear faulting were formed along the periphery of the imprint. Even at a higher load of 63.3 N (6.45 kg), the strengthened surface showed only an increase in the local shear faulting within the indentation. At approximately the same load levels, 13.2 N (1.35 kg) and 50.0 N (5.10 kg), respectively, the raw surface exhibited extensive radial and lateral cracking, despite being at slightly lower loads. It should be noted that static hardness measurements on the raw glass were not possible above 19.6 N (2 kg) due to significant cracking; however, the

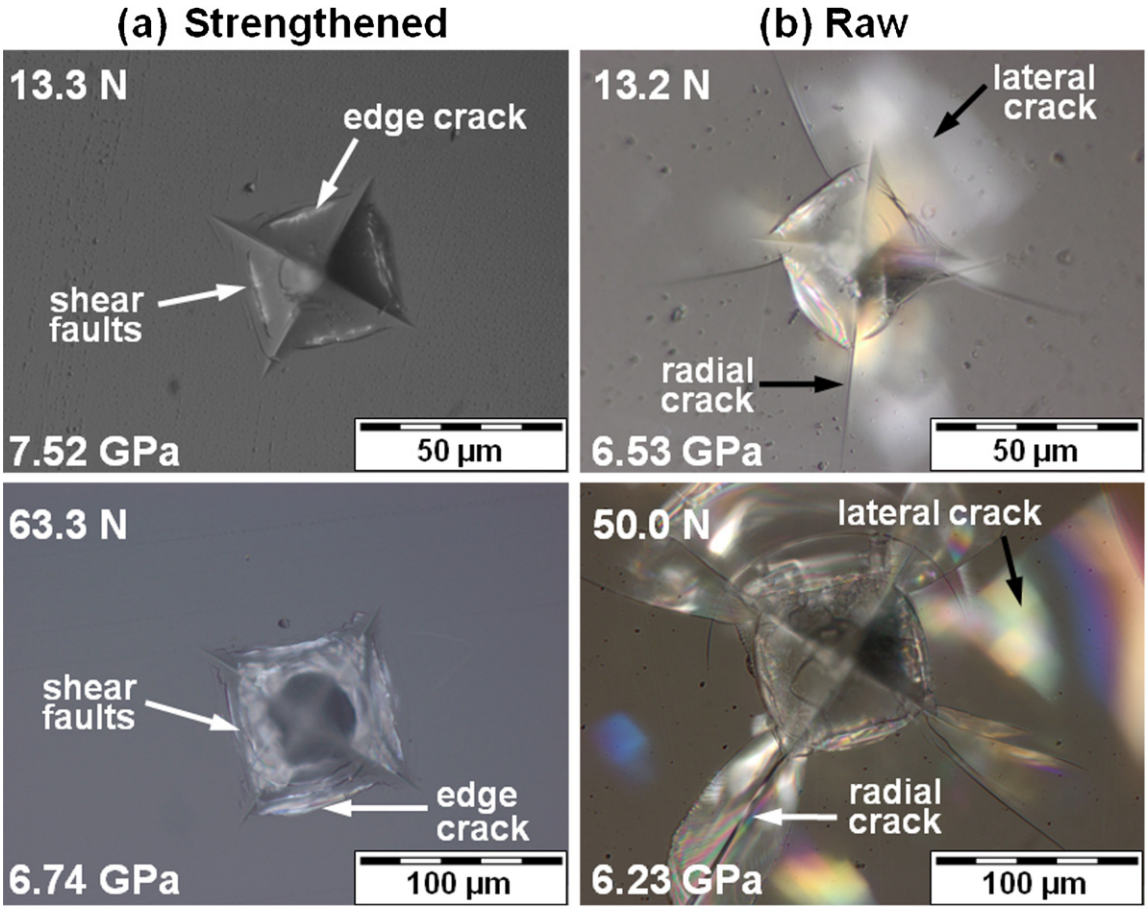


Fig. 5. Micrographs of dynamic Vickers indents on the (a) strengthened and (b) raw glass surfaces at comparable loads. Each micrograph includes the indentation load (top) as well as the Vickers hardness value (bottom) for that load. Note the lower level of damage on the strengthened glass compared to severe damage levels on the raw glass.

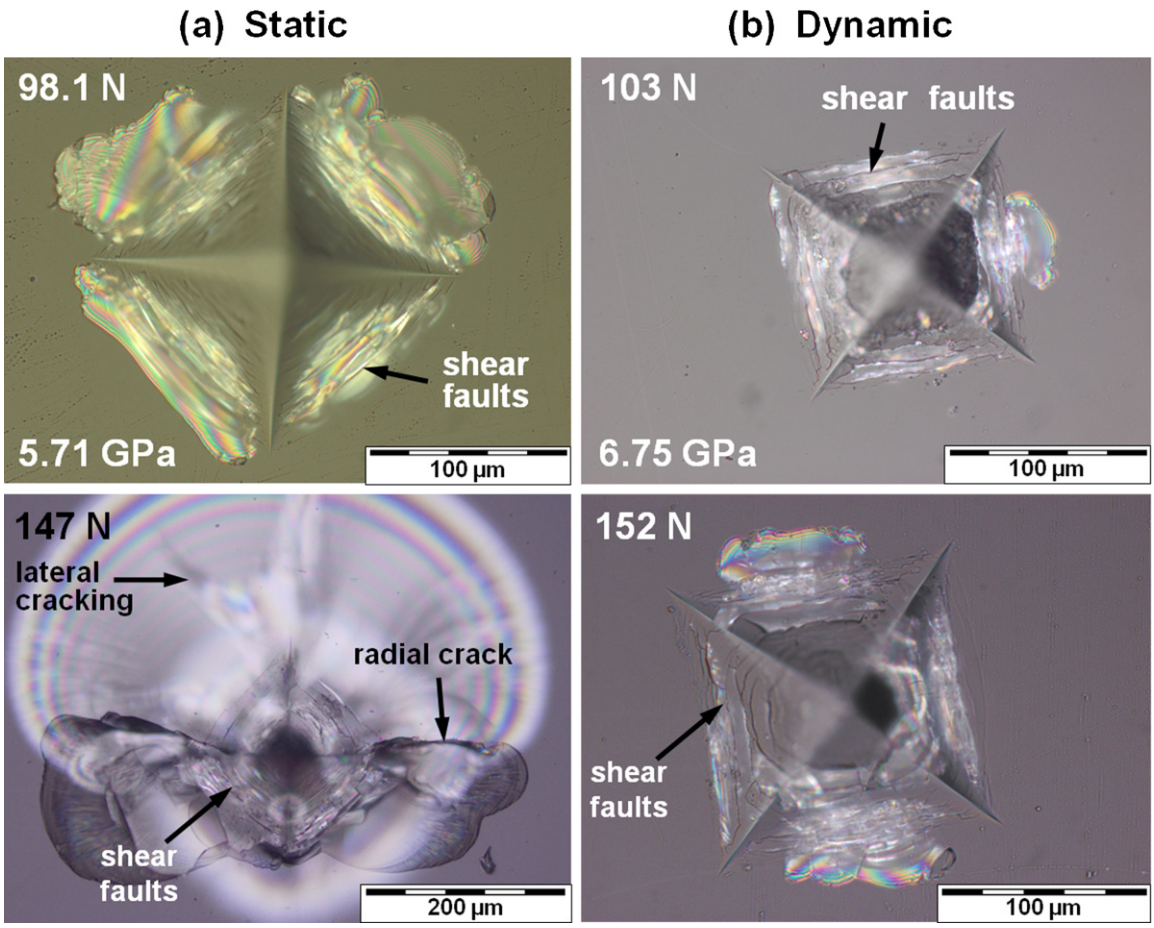


Fig. 6. Micrographs of indentation-induced damage on strengthened glass under (a) static and (b) dynamic loading at comparably high load levels. Included on each micrograph is the indentation load (top) as well as the hardness value at that load, if measured (bottom). Note the significant reduction in indent size and damage for dynamic indentation compared to static indentation even when the dynamic load is greater than the static load.

severity of the observed cracking under dynamic loading was significantly reduced and indents were measurable up to 112 N (11.4 kg). Clearly, an enhancement in crack resistance due to the chemical strengthening process and increased strain rate was evident.

Although it is typical to observe the evolution of radial crack systems emanating from the corners of Vickers indentation impressions (Figs. 4(b) and 5(b)) in brittle materials such as glass,[33] the high level of residual compressive stress present on the strengthened surface suppressed radial crack formation up to 147 N (15 kg) under static indentation and for all load ranges examined under dynamic indentation. Therefore, shear deformation mechanisms must be operative to cause plastic deformation in the strengthened glass in the form of shear faults. Unlike the raw glass which showed extensive radial and lateral cracking at moderate loads, the strengthened glass illustrated the obvious benefits of the ion exchange treatment. In Fig. 6 micrographs of Vickers indents at comparably high load levels are given to illustrate the effectiveness of the Ion-Armor$^{TM}$ glass in resisting indentation-induced fracture (especially radial cracking) under high static and dynamic loads. Vickers indents on the strengthened surface remained easily measurable and exhibited only moderate damage at static loads up to 98.1 N (10 kg) and at all examined dynamic loads ranges. Beyond 98.1 N (10 kg), static indentations exhibited notable cracking which made diagonal measurements impractical. Once a load level of 147 N (15 kg) was reached, radial crack formation was observed. As it has been proposed by Hagan[34] and Lawn et al.[35] that shear faults are sources of median, radian and lateral cracking, it is clear that the ultra-high surface compressive stresses acted to inhibit surface crack initiation (most notably radial cracking). As radial cracks are commonly viewed as strength-limiting flaws, the critical indentation load threshold at which radial cracking is observed can be viewed as an important parameter for materials design. This type of information is useful in quantifying the beneficial fracture resistance offered by ion exchanged glass.

In order to evaluate the influence of varying stress state on damage evolution, the cracking patterns due to Vickers indentations were analyzed on the unstrengthened surface at various depths from the strengthened surface within the tensile and compressive zones. Due to the beneficial compressive stresses present up to a depth of 0.8 mm (see Fig. 1(b)), the damage patterns within the compressive zone showed reduced indentation-induced cracking compared to the raw glass surfaces. However, for indentations performed within the central tensile region, the indentation-induced cracking was more significant (not shown

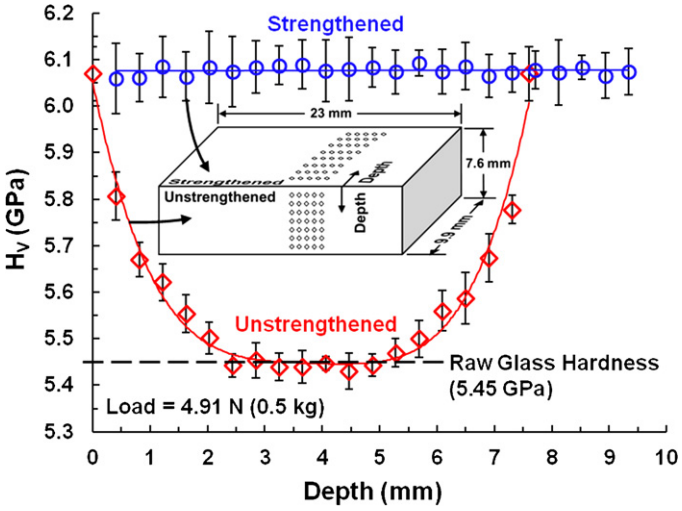


Fig. 7. Variation in static hardness with depth from edge-to-edge on the strengthened and the unstrengthened surfaces. The measurements on the strengthened surface revealed a constant hardness value whereas the measurements on the unstrengthened surface showed higher hardness values close to the edge and lower values in the central region.

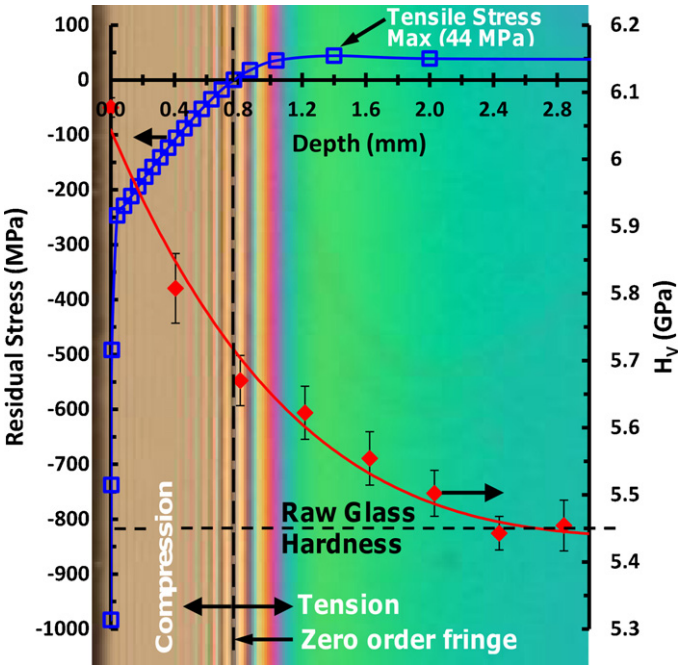


Fig. 8. Isochromatic fringe patterns near the edge of unstrengthened surface with hardness and residual stress data superimposed.

for brevity). The findings presented here agree well with previous studies,[36–38] as the crack growth and severity were shown to be initially reduced near the material surface due to the high compressive stresses, and as the depth increased toward the central region of the specimen, crack growth was less inhibited. Clearly, this behavior indicated that the hardness of the material could also be predicted to vary as a function of the depth from the outer compressive surface as presented in this investigation.

### 4.3. Variation of hardness with depth

The ion exchange process resulted in high residual compressive stresses on the surface and a severe stress gradient with depth below the strengthened surfaces. The stress state is tensile in the interior region (see Fig. 1(b)) so as to satisfy overall equilibrium conditions. For this reason, it is of particular interest to explore the spatial variation of mechanical properties as a function of depth on both the strengthened and the unstrengthened surfaces (see Fig. 7). Recall that the glass specimens being investigated in this study are only partially surface strengthened, because select surfaces (referred to as the "unstrengthened" surfaces in Figs. 1 and 7) have been polished to remove the strengthened layer so as to expose the subsurface material. In order to examine the influence of the strengthening treatment and the depth up to which the hardness is improved, static Vickers hardness measurements were conducted across the entire length of the strengthened and unstrengthened surfaces as illustrated in the inset of Fig. 7.

Hardness measurements shown in Fig. 7 on the strengthened surface show that the hardness remained constant around 6.08 GPa from one edge to the other. This indicated that the strengthening process resulted in consistent improvement to the properties across the entire strengthened surface compared to the raw glass hardness of 5.45 GPa. This is expected as the residual stress on the surface is uniform in magnitude and varies only with depth below the strengthened surface. On the contrary, the hardness profile on the unstrengthened surface showed higher hardness values at the edges and lower values in the interior region. The latter set of measurements also revealed that the hardness remained constant in the interior region of the lateral surface at the same hardness as that of the raw glass. Thus, from the interior of the glass (5.45 GPa), a steep increase in hardness was observed beginning from a depth of almost 2.4 mm below the strengthened surface, eventually reaching the strengthened glass hardness of 6.08 GPa at the surface. This trend indicates that the residual compressive stress beneath the strengthened surface causes higher hardness close to the surface and with increasing depth the hardness decreased as the stress state became more tensile. This hardness profile is consistent with the reported typical residual stress profiles in tempered glass.[21,39,40]

### 4.4. Photoelasticity

To further quantify the relationship between the residual stress state and the indentation hardness, photoelasticity was employed. When polarized light passes through a birefringent material (such as glass), the light is split into two different wave fronts, each oriented parallel to a principal stress direction and traveling at a different velocity.[38,41] Using a circular polariscope, the resulting fringe patterns were correlated to residual stress levels and related to the hardness as shown in Fig. 8. As detailed in Jannotti et al.,[19] the overall residual stress profile in the bulk specimen can be determined using a thick specimen and a typical polariscope, but a thin specimen and high magnification optics are required to determine the ultra-high compressive stress levels near the edges (within tens of microns). The entire residual stress

profile is shown in Fig. 8 with open square symbols. Jannotti et al.[19] determined the compressive stress level on the strengthened surface to be close to 1 GPa, decreasing rapidly to less than 300 MPa within 25 μm. The stress profile gradually tended to zero in the bulk specimen at a depth of 0.8 mm from the surface where the zero order fringe is indicated. Beyond this depth the residual stress state becomes tensile in the glass interior and approximately constant at 37 MPa.

The subsurface hardness profile (Fig. 7) was superimposed with the stress profile onto the photoelastic fringe patterns (see Fig. 8). By superposing both the trends in the residual stress state and the hardness, the depth to which the beneficial improvements in hardness over the raw glass hardness can be determined. Due to the severe residual stress gradient beneath the strengthened surface, it was expected that the hardness would show a strong variation with depth below the strengthened surface. From Fig. 8, it is clear that the residual compressive stress zone induced by chemical treatment extends only to a depth of 0.8 mm (from photoelasticity); however, the depth to which the hardness is improved over the raw glass hardness is around 2.4 mm. These results suggest that improvements in apparent hardness due to the ion exchange process extend to around 3 times the depth of the compressive stress layer. However, just beyond the zero stress fringe, prior to the tensile stress becoming constant, there existed an anomalous tensile maximum (at 1.5 mm depth) which stretched to slightly more than 2 mm, the depth at which the hardness was observed to stabilize to the same level as that of the raw glass (see Fig. 8). The presence of this anomalous tensile maximum in ion-exchanged glass is well-documented in the literature,[39,42–45] but there is no unified conclusion with regards to its existence. Based on this observation, it is speculated that the wedging of larger $Na^+$ and $K^+$ ions into the Li-glass causes a significant plastic stretch of the underlying substrate structure. Hence, it is feasible that the effect of these foreign alkali ions extended well beyond the case depth. While these arguments are purely speculative at present, more systematic analysis (such as molecular dynamics calculations) may be warranted to further validate these notions.

## 5. Conclusion

Static and dynamic Vickers indentation experiments on the strengthened and raw glass surfaces revealed notable ISE and rate-sensitivity in hardness. The hardness of the strengthened glass was 11% higher than the raw glass under static and dynamic loading as a result of the ion exchange treatment. The dynamic hardness values of both the strengthened and the raw glass surfaces showed an increase over the static hardness values due to increased strain rate (23% and 22%, respectively). Additionally, the strengthened surface exhibited a suppression of radial cracking for static loads up to 147 N (15 kg) and for all dynamic loads examined. For the raw glass, lateral and radial cracking was observed to initiate at very low loads and become increasingly more severe with increasing load levels. However, the strengthened and raw glass surfaces both showed a significant increase in crack resistance at high loading rates. With regards to the hardness profiles on the strengthened and unstrengthened glass surfaces, the hardness on the strengthened surface remained constant across the entire surface at about 6.08 GPa, and subsurface hardness values (on the unstrengthened surface) exhibited improved hardness values until a depth of 2.4 mm was reached. At this point, the hardness became constant at 5.45 GPa, which is equivalent to the raw glass hardness. This means that although the residual compressive stress layer only extended to 0.8 mm depth, the hardness remained above the raw glass hardness up to a depth of 2.4 mm. Thus, the influence of the ion exchange process was found to extend well beyond the residual compression zone, to about 3 times the measured case-depth.

## References


1. Varshneya AK, Spinelli IM. High-strength, large-case-depth chemically strengthened lithium aluminosilicate glass. *Am Ceram Soc Bull* 2009;**88**:213–20.
2. Varshneya AK. Chemical strengthening of glass: lessons learned and yet to be learned. *Int J Appl Glass Sci* 2010;**1**:131–42.
3. LaSalvia JC. A physically-based model for the effect of microstructure and mechanical properties on ballistic performance. In: Lin H-T, Singh M, editors. *26th annual conference on composites, advanced ceramics, materials, and structures: A, ceramic engineering and science proceedings, vol. 23, issue 3*. John Wiley & Sons, Inc.; 2002. p. 213–20.
4. LaSalvia JC. Recent progress on the influence of microstructure and mechanical properties on ballistic performance. *Ceram Trans* 2002;**134**:557–70.
5. Anderson CE, Royal-Timmons SA. Ballistic performance of confined 99.5%-$Al_2O_3$ ceramic tiles. *Int J Impact Eng* 1997;**2**:703–13.
6. Pereira JM, Lerch BA. Effects of heat treatment on the ballistic impact properties of Inconel 718 for jet engine fan containment applications. *Int J Impact Eng* 2001;**25**:715–33.
7. Woodward RL, Baxter BJ. Ballistic evaluation of ceramics: influence of test conditions. *Int J Impact Eng* 1994;**15**:119–24.
8. Orgaz F, Gomez-Del Rio T. Dynamic fracture and fragmentation patterns of borosilicate laminate glasses. *Bull Span Soc Ceram Glass* 2009;**48**:267–72.
9. Karandikar PG, Evans G, Wong S, Aghajanian MK, Sennett M. A review of ceramics for armor applications. In: Franks LP, editor. *Advances in ceramic armor IV: ceramic engineering and science proceedings, vol. 29, issue 6*. John Wiley & Sons, Inc.; 2009. p. 163–75.
10. Chheda M, Normandia MJ, Shih J. Ceramic defense: improving ceramic armor performance. *Ceram Ind* 2006;**12**:124–46.
11. Subhash G. Dynamic indentation testing. In: Kuhn H, Medlin D, editors. *ASM handbook on mechanical testing and evaluation*, vol. 8. Materials Park, OH: ASM International; 2000. p. 519–29.
12. Anton RJ, Subhash G. Dynamic Vickers indentation of brittle materials. *Wear* 2000;**239**:27–35.
13. Kese KO, Li ZC, Bergman B. Influence of residual stress on elastic modulus and hardness of soda-lime glass measured by nanoindentation. *J Mater Res* 2004;**19**:3109–19.
14. Botvinkin OK, Denisenko ON. Application of ion exchange method to increase the hardness of polished glass. *Glass Ceram* 1968;**25**:78–80.
15. Haney EJ, Subhash G. Static and dynamic indentation response of basal and prism plane sapphire. *J Eur Ceram Soc* 2011;**31**:1713–21.
16. Haney EJ, Subhash G. Analysis of interacting cracks due to sequential indentations on sapphire. *Acta Mater* 2011;**59**:3528–36.
17. Klecka MA, Subhash G. Rate-dependent indentation response of structural ceramics. *J Am Ceram Soc* 2010;**93**:2377–83.
18. Ghosh D, Subhash G, Sudarshan TS, Radhakrishnan R, Gao X. Dynamic indentation response of fine-grained boron carbide. *J Am Ceram Soc* 2007;**90**:1850–7.
19. Jannotti P, Subhash G, Ifju P, Kreski PK, Varshneya AK. Photoelastic measurement of high stress profiles in ion-exchanged glass. *Int J Appl Glass Sci* 2011;**2**:275–81.
20. Abrams MB, Green DJ, Glass SJ. Fracture behavior of engineered stress profile soda lime silicate glass. *J Non-Cryst Solids* 2003;**321**:10–9.

21. Green DJ, Tandon R, Sglavo VM. Crack arrest and multiple cracking in glass through the use of designed residual stress profiles. *Science* 1999;**283**:1295–7.
22. Klecka MA, Subhash G, Arakere NK. Determination of subsurface hardness gradients in plastically graded materials via surface indentation. *J Tribol* 2011;**133**:031403.
23. Cavaliere P, Zavarise G, Perillo M. Modeling of the carburizing and nitriding processes. *Comput Mater Sci* 2009;**46**:26–35.
24. Nemat-Nasser S, Isaacs JB, Starrett JE. Hopkinson techniques for dynamic recovery experiments. *Proc R Soc of Lond A: Math Phys Sci* 1991;**435**:371–91.
25. Alcalá J, Barone AC, Anglada M. The influence of plastic hardening on surface deformation modes around Vickers and spherical indents. *Acta Mater* 2000;**48**:3451–64.
26. Knoop F, Peters CG, Emerson W. A sensitive pyramidal-diamond tool for indentation measurements. *J Res Nat Bur Stds* 1939;**23**:39–61.
27. Peters CG, Knoop F. Resistance of glass to indentation. *Glass Ind* 1939;**20**:174–6.
28. Quinn J, Quinn G. Indentation brittleness of ceramics: a fresh approach. *J Mater Sci* 1997;**32**:4331–46.
29. Swab JJ. Recommendations for determining the hardness of armor ceramics. *Int J Appl Ceram Technol* 2004;**1**:219–25.
30. Li H, Bradt RC. The indentation load/size effect and the measurement of the hardness of vitreous silica. *J Non-Cryst Solids* 1992;**146**:197–212.
31. Sargent PM. Use of the indentation size effect on microhardness for materials characterization. In: Blau PJ, Lawn BR, editors. *Microindentation techniques in materials science and engineering, ASTM STP 889*. Philadelphia, PA: American Society for Testing and Materials; 1986. p. 160–74.
32. Tóth Z, Nagy A, Steinbach G, Juhász A. Investigation of indentation-caused cracking in surface-modified silica glasses. *Mater Sci Eng A* 2004;**387–389**:542–5.
33. Cook RF, Pharr GM. Direct observation and analysis of indentation cracking in glasses and ceramics. *J Am Ceram Soc* 1990;**73**:787–817.
34. Hagan JT. Shear deformation under pyramidal indentations in soda-lime glass. *J Mater Sci* 1980;**15**:1417–24.
35. Lawn BR, Dabbs TP, Fairbanks CJ. Kinetics of shear-activated indentation crack initiation in soda-lime glass. *J Mater Sci* 1983;**18**:2785–97.
36. Morris DJ, Myers SB, Cook RF. Indentation crack initiation in ion-exchanged aluminosilicate glass. *J Mater Sci* 2004;**39**:2399–410.
37. Lawn BR, Marshall DB, Wiederhorn SM. Strength degradation of glass impacted with sharp particles: II, tempered surfaces. *J Am Ceram Soc* 1979;**62**:71–4.
38. Hearn EJ. *Mechanics of materials 2: an introduction to the mechanics of elastic and plastic deformation of solids and structural materials*. 3rd ed. Oxford: Butterworth-Heinemann; 1997. p. 184.
39. René G. Ion exchange for glass strengthening. *Mater Sci Eng B* 2008;**149**:159–65.
40. Sglavo VM, Bonafini M, Prezzi A. Procedure for residual stress profile determination by curvature measurements. *Mech Mater* 2005;**37**:887–98.
41. Sharpe WN. *Springer handbook of experimental solid mechanics*. Boston, MA: Springer Science/Business Media; 2008. p. 701.
42. Varshneya AK, Petti RJ. Finite element analysis of stresses in ion-exchanged glass. *J Am Ceram Soc* 1976;**59**:42–6.
43. Sane AY, Cooper AR. Anomalous stress profiles in ion-exchanged glass. *J Am Ceram Soc* 1978;**61**:359–62.
44. Tyagi V, Varshneya AK. Measurement of progressive stress buildup during ion exchange in alkali aluminosilicate glass. *J Non-Cryst Solids* 1998;**238**:186–92.
45. Schaeffer HA, Heinze R. Stress buildup by ion exchange of glasses. *Glastech Ber* 1974;**47**:199–207.